Chapter

Carbothermal Synthesis of Spherical AlN Fillers

Qi Wang, Kexin Chen and Wenbin Cao

Abstract

Micro-sized spherical AlN particles have presented great commercial potential as thermally conductive fillers for high-performance thermal interface materials, benefiting from their high thermal conductivity and good fluidity in the polymers. In this chapter, recent research progress in the carbothermal synthesis of spherical AlN fillers is highlighted. The influences of various synthetic parameters, including N_2 gas pressure, additive content, additive particle size, reaction temperature, reaction time, carbon content, and additive types, on the nitridation rate and the particle size and morphology of final AlN powders are summarized. More importantly, the growth mechanism of micro-sized spherical AlN granules is deeply discussed as well.

Keywords: carbothermal synthesis, spherical AlN particles, thermally conductive fillers, thermal interface materials, growth mechanism

1. Introduction

With the rapid progress of microelectronics technology, electronic products and devices are developing toward the direction of miniaturization and high integration. Although powerful functions are introduced, the heat dissipation has become an important bottleneck restricting the development of electronic technology. In the field of heat dissipation, thermal interface materials (TIMs) play an important role. TIMs are mainly used to fill the microvoids or uneven holes generated by the contact between heating devices and radiators, establishing an effective channel and improving the efficiency of heat dissipation [1]. Therefore, the TIMs are receiving more and more attention.

In order to achieve optimum heat dissipation, the TIMs should have good ductility to fill the air gap completely. Polymeric materials have attracted increasing interest owing to their excellent processability, high ductility, and low cost. However, most of the polymers have thermal conductivity lower than 0.5 W/m K [2], which is difficult to meet the demand for heat dissipation. To solve this problem, one effective approach is to introduce high–thermal-conductivity fillers into the polymers. Inorganic ceramic powders have been considered as ideal fillers benefiting from their high thermal conductivity, low dielectric constant, and good insulating properties. At present, oxides and nitrides are the most commonly considered fillers.

Silica (SiO_2) is widely used in the field of electronic heat dissipation because of its safety, reliability, and low cost [3, 4]. However, its intrinsic thermal conductivity is only 1.5–1.6 W/m K [5], so it is difficult to obtain composite materials with higher

thermal conductivity. Zinc oxide (ZnO) has a high thermal conductivity up to 60 W/m K, but the high dielectric constant greatly restricts its practical application as fillers [6]. Beryllia (BeO) has the highest thermal conductivity (~240 W/m K) in all the inorganic oxides. However, the high cost and high toxicity make it unattractive for commercial use [5]. Comparatively, alumina (Al_2O_3) has a much higher thermal conductivity than SiO_2 and also presents remarkable electrical and mechanical properties, as well as the cheap producing cost [7–9], so it is the most widely used commercial filler at present. Kozato et al. [7] successfully prepared epoxy composites filling with 60 vol% Al_2O_3, achieving a high thermal conductivity of 4.3 W/m K. However, due to the relatively low intrinsic thermal conductivity of 38~42 W/m K [5], it is still difficult for Al_2O_3 to prepare high-performance TIMs to satisfy the increasing heat-dissipation requirements in future.

Compared with oxides, nitride powders are more attractive owing to the relatively high thermal conductivity. For example, boron nitride (BN) has a thermal conductivity as high as 280 W/m K and also shows the stable chemical property [10]. Xu et al. [11] used modified BN particles as fillers and finally prepared the composites with a high thermal conductivity of 10.3 W/m K. Nevertheless, the high price still limits its wide application. Silicon nitride (Si_3N_4) has a low coefficient of thermal expansion and a low dielectric constant, but it has been seldom used as fillers for high-thermal conductivity TIMs owing to its moderate thermal conductivity of 86~120 W/m K [12].

In comparison, aluminum nitride (AlN) has attracted tremendous attention in the electronic industry thanks to its outstanding properties such as high intrinsic thermal conductivity (~320 W/m K), good electrical resistivity, low dielectric constant, and low thermal expansion coefficient close to that of silicon [13, 14]. Ohashi et al. [15] filled epoxy resin with 74 vol% approximately spherical AlN particles, obtaining a composite thermal conductivity as high as 8.2 W/m K. Zhou et al. [16] prepared TIMs using angular AlN powders to replace Al_2O_3, and the composite thermal conductivity was increased to 2.6 times with a filling fraction of 68.5 vol%. Therefore, AlN fillers have shown prosperous application prospects for preparing high-performance TIMs.

Besides the intrinsic thermal conductivity of fillers, the thermal properties of TIMs are also affected by the filling fraction, the shape and particle size of fillers. In order to prepare the composites with higher thermal conductivity, it is important to raise the filler loading as high as possible and meanwhile retain the good fluidity of the composites for facile processability [17]. Compared with angular and plate-like particles, spherical fillers offer greater advantages in this regard owing to their better fluidity in the polymers [2]. In addition, it is generally believed that the thermal conductivity of composites increases with increasing the particle size of fillers [18]. This can be explained by the following two reasons: on the one hand, larger particles tend to result in the smaller fillers/matrix interfaces, leading to less photon scattering and lower thermal resistance; on the other hand, the fillers with a larger particle size are more easy to achieve higher filling fraction owing to the better fluidity and lower viscosity of the fillers/matrices. In general, the micro-sized fillers can give higher composite thermal conductivity than nano-sized fillers. Therefore, with the above considerations in mind, it is great significant and imperative to synthesize micro-sized spherical AlN particles as thermally conductive fillers for the next generation TIMs.

Despite the potentially high commercial importance, the large-scale synthesis of micro-sized spherical AlN fillers remains a huge challenge to date since nitrides tend to decompose at high temperature and cannot be converted to a spherical morphology just by the traditional surface tension method [19]. Up to now, limited related literatures can be retrieved. Among the existing studies, Ohashi et al. [15]

successfully synthesized spherical AlN particles via solution-reprecipitation treatment of angular AlN powders in a low-melting Ca-Al-O flux. Nevertheless, the particle size of the products was limited by the raw AlN powders, and the necessary hydrochloric acid treatment for removing residual Ca-Al-O was harmful to the product purity and the environment as well. Chowdhury et al. [20] first prepared core-shell structured C@Al_2O_3 composited particles, following the nitridation process in the flowing nitrogen at high temperature to ultimately obtain spherical AlN particles. However, the sphericity of the final product is very low due to the limitation of the heterogeneous mixing process. Suehiro et al. [21] synthesized spherical AlN particles by gas nitridation of spherical Al_2O_3, using a NH_3-C_3H_8 gas mixture as the reduction-nitridation agent, but the undesired impurities were still presented owing to the incomplete conversion. In addition, an effective two-step method, involving the freezing granulation and subsequent sintering process, was also developed to prepare spherical AlN granules with the high sphericity and particle size more than tens of microns [22, 23]. Nevertheless, the AlN was used as raw materials, resulting in the relatively high production cost. Therefore, it is still highly desirable to explore suitable methods to directly synthesize spherical AlN fillers with high sphericity and enhanced properties.

In general, commercial AlN powders are mainly synthesized by two methods. One is the direct nitridation of aluminum powders with N_2 or NH_3 ($2Al + N_2 \rightarrow 2AlN$); the other one is carbothermal reduction nitridation (CRN) of alumina powders in the presence of N_2 ($Al_2O_3 + 3C + N_2 \rightarrow 2AlN + 3CO$) [24]. Comparatively, the CRN method is a better choice for industry production since the resultant AlN powders exhibit more attractive properties such as high purity, facile sinterability, and resistance against humidity.

To date, many efforts have been devoted to ameliorating the quality of AlN powders synthesized by the CRN method [25–28]. Unfortunately, most of them just aimed at fabricating fine or ultrafine AlN powders via low-temperature synthesis to improve the sintering ability and reduce the fabricating cost. The obtained nano or submicron particles are too small to meet the basic requirements as promising fillers. Until recently, increasing attention has been paid on the carbothermal synthesis of coarser AlN granules, especially micro-sized spherical AlN fillers. Based on a series of studies [29–33], the authors have successfully synthesized micro-sized spherical AlN fillers by using appropriate additives and high-pressure N_2 in the CRN process. The as-synthesized AlN granules presented high sphericity, uniform size distribution, and good dispersing behavior, which exhibited great potential as high-performance thermally conductive fillers. Based on this, this chapter will focus on the research progress in the carbothermal synthesis of spherical AlN fillers. The influence of various synthetic parameters on the morphology and particle size of final products will be summarized, and the growth mechanism of micro-sized spherical AlN particles will be discussed as well.

2. Influence of carbothermal synthetic parameters

The typical carbothermal process for synthesizing spherical AlN fillers consists of three steps: first, the raw materials (Al_2O_3, carbon black, and additives) were homogenized by ball milling; second, the CRN process was conducted in a graphite furnace with a high temperature and an elevated N_2 gas pressure; finally, the obtained powders were transferred to a muffle oven and heated in air to remove the residual carbon. It was found that various synthetic parameters, such as N_2 pressure, additives, reaction temperature, reaction time, and carbon content had an important impact on the nitridation rate, the morphology, and the particle size of the final products.

2.1 Effects of N_2 gas pressure

In order to evaluate the effects of N_2 gas pressure on the nitridation rate and the morphology of AlN particles, the raw mixtures containing 5 wt.% CaF_2 additive were heated at a temperature ranging from 1400 to 1800°C and under various N_2 pressure (0.1, 0.1, and 1 MPa), respectively. The AlN conversion fraction was determined based on XRD peak intensities of the plane (100) of AlN and (104) of Al_2O_3. **Figure 1** shows the relationship between AlN conversion fraction and N_2 pressure at various reaction temperatures.

As observed, AlN conversion fraction was significantly decreased with increasing the N_2 pressure, indicating an elevated N_2 pressure hampered the reduction-nitridation process. Based on the studies of Forslund et al. [34, 35], under a high N_2 pressure, the removal of produced CO vapor became more difficult. Thus, a barrier was set up on the surface of solid raw materials by the increased CO level, which limited the contact between Al_2O_3 and N_2, and eventually decreased the reduction-nitridation rate. In addition, it can also be observed in **Figure 1** that the nitridation rate increased with the reaction temperature. When the reaction temperature was higher than 1600°C, the nitridation rate was significantly improved due to the high reaction activity. As a result, Al_2O_3 was completely converted into AlN irrespective of the tested N_2 pressure values.

Figure 2 further presents the SEM images of the AlN powders synthesized at 1800°C but under various N_2 pressures. Under the N_2 pressure of 0.1 Mpa, as shown in **Figure 2a**, irregular AlN particles were obtained. When the N_2 pressure was increased to 0.5 Mpa, approximately spherical AlN particles could be observed in **Figure 2b**. With the N_2 pressure further increasing to 1 Mpa, micro-sized spherical AlN fillers were successfully prepared, as shown in **Figure 2c**. It should be noted that the both particle size and the sphericity of the as-synthesized AlN particles were improved with increasing the N_2 pressure. As established, the elevated N_2 pressure tended to improve the CO level in the system. The AlN nucleation rate was slowed down, resulting in the large particle size. Additionally, CaF_2 additive was expected to react with Al_2O_3 to form low-melting Ca-aluminates, providing the liquid catalyst for AlN nucleation [36]. The slow reaction rate under the elevated N_2 pressure was also beneficial for the migration and uniform distribution of Ca-aluminate liquid phases in the system. Therefore, the uniform liquid-assisted

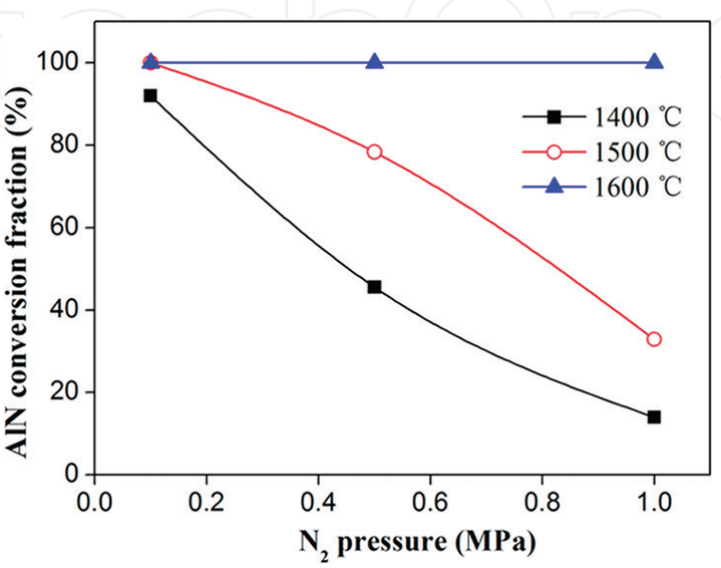

Figure 1.
Relationship between AlN conversion fraction and N_2 gas pressure at various reaction temperatures [31].

nucleation further promoted the formation of AlN particles with the larger particle size, uniform distribution, and spherical morphology.

2.2 Effects of additive content

As mentioned above, the aluminates formed from the reaction between additives and Al_2O_3 played an important role to determine the CRN reaction rate and the morphology of AlN particles. Therefore, the investigation of the additive was helpful to verify the previous inference and better understand the formation mechanism of spherical AlN particles. In this section, the raw materials with various CaF_2 contents (0, 3, 5, and 10 wt.%) were used to proceed the CRN reaction under the high N_2 pressure of 1 MPa and at different temperatures of 1500 and 1800°C. The XRD patterns of the as-synthesized products were shown in **Figure 3**.

As observed from **Figure 3a**, Al_2O_3 was identified in all samples, indicating the incomplete nitridation at 1500°C. In the absence of CaF_2, the peaks of Al_2O_3 were detected strongly. When 3 wt.% CaF_2 was introduced, the relative intensity of the Al_2O_3 diffraction peaks decreased obviously, which indicated that a small amount of CaF_2 could effectively accelerate the nitridation rate. However, with the CaF_2 content further increased to 5 and 10 wt.%, the peaks of Al_2O_3 increased instead, suggesting the conversion fraction of AlN was decreased. This is mainly because the reaction between CaF_2 and Al_2O_3 was relatively slow at the low temperature of 1500°C; excessive and unreacted CaF_2 existed in the system, hindering the contact between reactants and further retarding the nitridation process [37]. In addition, the secondary phase of $CaAl_{12}O_{19}$ was detected in all samples with CaF_2. The Ca-aluminates were mainly formed from the reaction between Al_2O_3 and CaF_2. The process can be described by the following equations [38]:

$$Al_2O_3(s) + 3CaF_2(s) \rightarrow 2AlF_3(g) + 3CaO(s) \quad (1)$$

$$CaO(s) + Al_2O_3(s) \rightarrow Ca\text{–aluminates (l)} \quad (2)$$

As the reaction proceeds, the low-melting Ca-aluminates tended to be reduced and further transformed into AlN, providing some Ca-compounds [39]:

$$Ca\text{–aluminates (l)} + C(s) + N_2(g) \rightarrow AlN(s) + CO(g) + Ca\text{–compounds} \quad (3)$$

The reduction and nitridation of intermediate Ca-aluminate liquid undergo an easier nitridation process, promoting the conversion rate from Al_2O_3 to AlN.

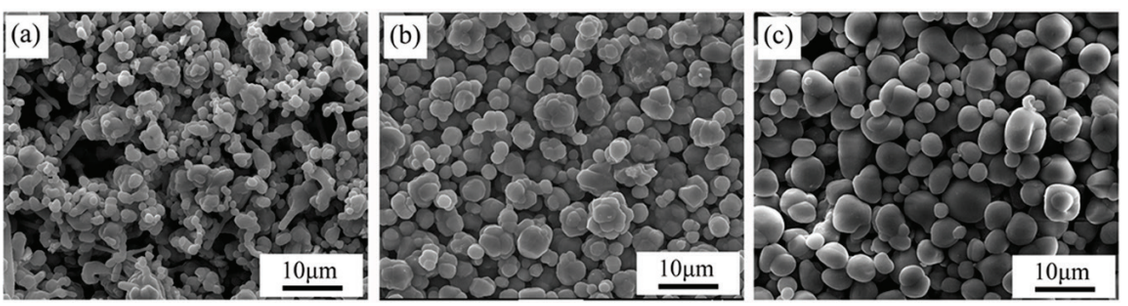

Figure 2.
SEM images of the AlN powders synthesized at 1800°C but under various N_2 pressures: (a) 0.1 Mpa, (b) 0.5 Mpa, and (c) 1 Mpa [31].

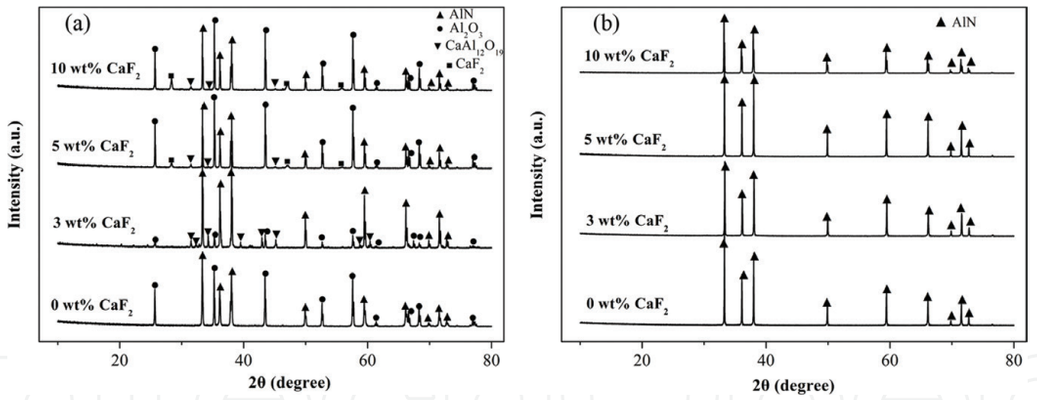

Figure 3.
XRD patterns of the products synthesized with various CaF_2 contents at (a) 1500°C and (b) 1800°C.

When the reaction temperature was increased to 1800°C, only the peaks of AlN were observed in **Figure 3b**, suggesting the full conversion of Al_2O_3 to AlN. Moreover, it is necessary to note that no diffraction peaks ascribed to the CaF_2 or Ca-compounds were detected, inferring that Ca-compounds were just formed at relatively low temperature; afterwards, they were reduced and further vaporized in the atmosphere with the increase of synthesis temperature. The process was established as follows [39, 40]:

$$\text{Ca–aluminates (l)} + \text{C(s)} + \text{N}_2\text{(g)} \rightarrow \text{AlN(s)} + \text{CO(g)} + \text{Ca(g)} \qquad (4)$$

Figure 4 further shows the SEM images of the AlN products synthesized at 1800°C. As observed in **Figure 4a**, small particles accompanied with some irregular grains were obtained in the absence of the CaF_2 additive. When a different amount of CaF_2 ranging from 1 to 10 wt.% was added, both the sphericity and particle size of AlN granules significantly increased with the CaF_2 content, as shown in **Figure 4b–d**. Clearly, the higher CaF_2 content meant more Ca-aluminate liquids were generated, providing the liquid environment for AlN nucleation and material transport. A large amount of Ca-aluminate liquid explicitly favored for the complete wrap of AlN particles, promoting the formation of a smooth spherical morphology. In addition, the small AlN particles were more easy to dissolve in the excessive liquid phase and reprecipitate on the surface of large particles, which finally promoted the growth of AlN particles via the dissolution-precipitation mechanism.

2.3 Effects of the additive particle size

In this section, CaF_2 granulations with different particle sizes (<75 μm, 75~150 μm, and >150 μm) were used to evaluate the effects of the additive particle size on the nitridation rate and morphology of the final products. The nitridation pressure in the CRN process was maintained at 1 MPa. According to the particle size of CaF_2 granulations changing from small to large, the obtained powders were briefly named as ACF-S, ACF-M, and ACF-L. **Table 1** summarized the AlN conversion fraction of the products synthesized at 1500 and 1800°C.

It could be clearly inferred that the AlN conversion fraction decreased with the increase of the CaF_2 particle size at the low temperature of 1500°C. This is mainly because the large CaF_2 particle size tended to reduce the reaction rate between CaF_2 and Al_2O_3, leading to the slow formation rate of Ca-aluminates. This observation further demonstrated that the Ca-aluminates played a central role in the nitridation process. When the temperature increased to 1800°C, full nitridation

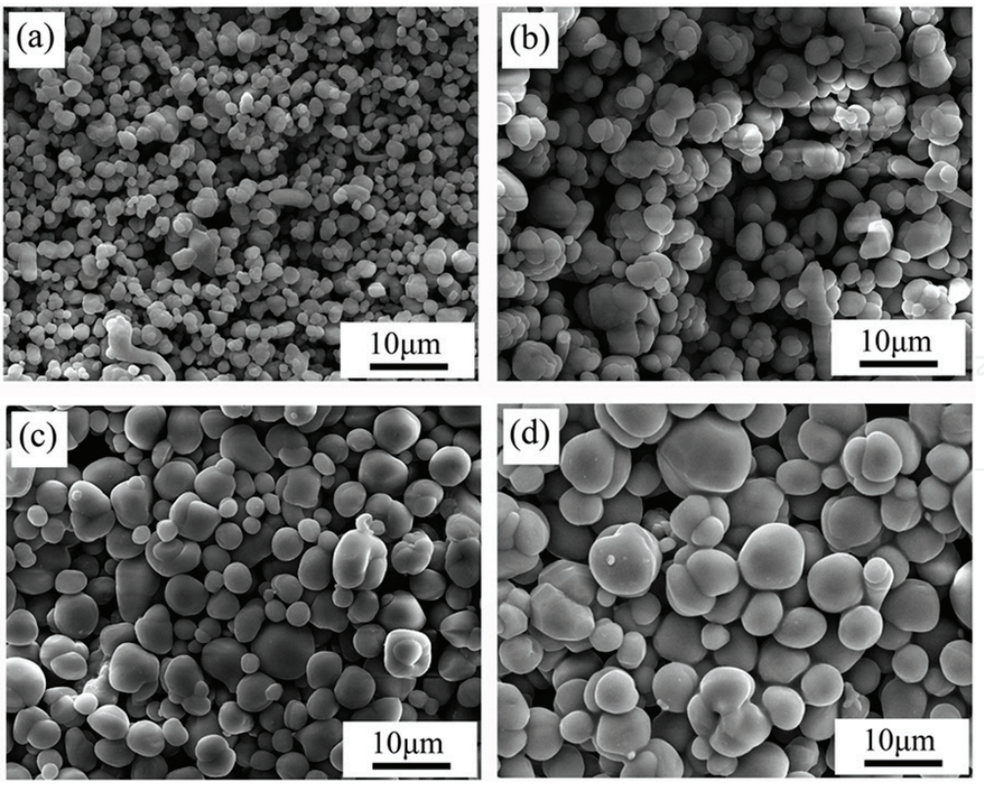

Figure 4.
SEM images of the AlN products synthesized at 1800°C with various CaF_2 contents: (a) 0, (b) 3, (c) 5, and (d) 10 wt.% [31].

Samples	CaF_2 particle size (μm)	AlN conversion fraction (%)	
		1500°C	1800°C
ACF-S	<75	88.03	100
ACF-M	75~150	73.01	100
ACF-L	>150	57.36	100

Table 1.
The AlN conversion fraction of the products synthesized with different CaF_2 particle sizes at 1500 and 1800°C [29].

was achieved for all samples, and the corresponding SEM images are shown in **Figure 5**.

As observed, the particle size of AlN products significantly decreased with increasing the particle size of the CaF_2 additive. As mentioned, the large CaF_2 particle size could lead to a low formation rate of liquid aluminates. Therefore, insufficient liquid aluminates existed in the system. As a result, small AlN particles were difficult to precipitate on the surface of large particles through the dissolution-precipitation mechanism. The rearrangement and growth of AlN particles were limited, leading to the AlN products with a small particle size.

2.4 Effects of reaction temperature

Figure 6 shows the typical SEM images of the AlN granules synthesized from a typical mixture of Al_2O_3/C with 5 wt.% CaF_2 at various reaction temperatures (1600–1900°C) under the N_2 pressure of 1 MPa for 2 h. As can be seen, the temperature has a great influence on the morphology and particle size of the as-synthesized AlN granules. At 1600°C, angular AlN granules along with several tadpole-like

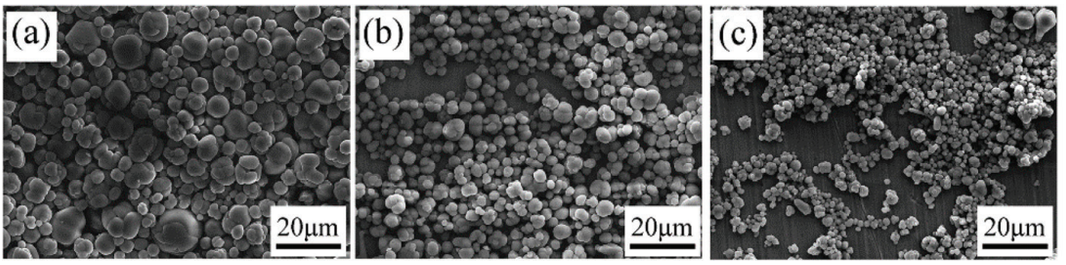

Figure 5.
SEM images of the products synthesized with different CaF_2 particle sizes at 1800°C: (a) ACF-S, (b) ACF-M, and (c) ACF-L [29].

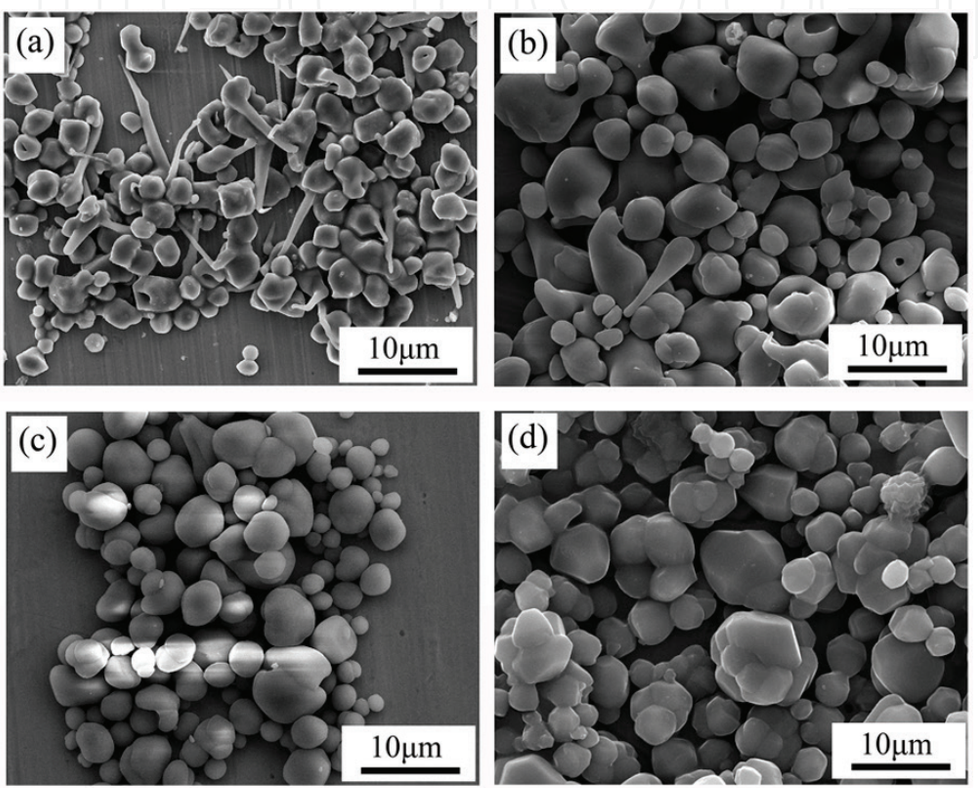

Figure 6.
SEM images of the AlN products synthesized at various temperatures: (a) 1600 [31], (b) 1700 [31], (c) 1800, and (d) 1900°C.

particles were obtained. As the temperature increased to 1700 and 1800°C, the tadpole-like morphology gradually disappeared, while the shape of AlN particles was changed from angular to spherical. However, when the temperature was further raised to 1900°C, the morphology was abnormal again, changing from spherical to angular.

This interesting observation can be understood from the formation and distribution of liquid aluminates. In general, two main reaction processes existed in the system: one is the formation process of Ca-aluminates through the reaction between Al_2O_3 and CaF_2, and the other one is the nitridation process of Ca-aluminates, promoting the formation of AlN. The low formation rate and the high nitridation rate of Ca-aluminates could both result in the reduced content of liquid phases in the system, which would obviously affect the morphology of AlN particles. At a low temperature of 1600°C, the Ca-aluminates appeared in a small amount and tended to distribute unevenly in the system due to the slow reaction rate between CaF_2 and Al_2O_3. As a consequence, AlN had a higher growth rate in the liquid concentration area, leading to the appearance of "tadpole tail." In addition, the small amount of liquid phases also resulted in a relatively slow material migration rate, thus the

AlN granules preferred growing into the angular morphology according to the crystal structure [41]. When the temperature was increased to 1700 and 1800°C, the amount of liquid Ca-aluminates remarkably increased. The rapid material migration aiding with the liquid phases eventually promoted the formation of the spherical morphology with the lowest surface free energy. However, when the temperature was further increased to 1900°C, the nitridation rate of liquid Ca-aluminates increased significantly, even larger than that of the formation rate. In other words, the Ca-aluminates were nitrided immediately as soon as they were formed. There were not enough liquid phases in the system to modify the morphology of AlN. As a result, AlN presented the angular morphology again in accordance with its own structure.

2.5 Effects of reaction time

To investigate the effects of reaction time on the morphology of AlN products, the raw materials with 5 wt.% CaF_2 were heated at 1800°C and under the N_2 pressure of 1 MPa for various reaction times (0.5, 1, 2, and 4 h). **Figure 7** shows the SEM images of the as-synthesized powders.

As the reaction time prolonging from 0.5 to 1 h and further to 2 h, the size and uniformity of AlN particles significantly increased. It was expected that the dissolution and reprecipitation of AlN aiding with liquid phases contributed greatly to the particle growth. In addition, as the prolongation of reaction time, the residual liquid phases in the system could also adjust themselves under the action of the interfacial energy to uniformly wrap the AlN particles, further improving the uniformity of the particle size. However, when the reaction time further increased to 4 h, the growth of AlN particles was no longer obvious. Instead, most of the AlN particles were sintered each other to form large aggregates, and the individual particles tended to change from the spherical to angular morphology, as demonstrated by the

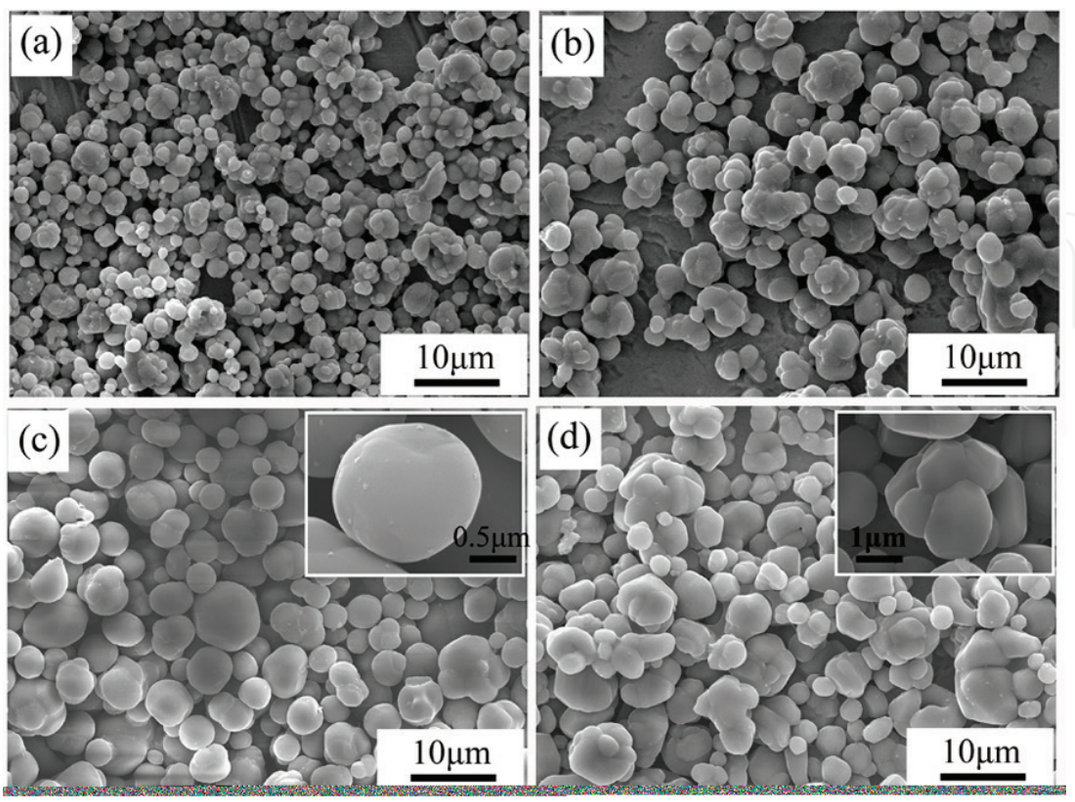

Figure 7.
SEM images of the AlN products synthesized for various reaction times: (a) 0.5, (b) 1, (c) 2, and (d) 4 h [29].

inserted images in **Figure 7c** and **d**. As the reaction proceeding, Ca-aluminates were continuously consumed until they were completely reduced to Ca vapor following Eq. (4). The residual liquid phase was too less to completely encapsulate the AlN particles. The driving force of small AlN particles migrating to large particles decreased, and the energy required for the growth of individual particles increased. Therefore, the AlN particle growth gradually stopped and was replaced by the neck sintering between particles.

2.6 Effects of the carbon content

It is generally believed that the ratio of carbon and Al_2O_3 has a great effect on the CRN process. Traditionally, excessive carbon was used to guarantee the full conversion of Al_2O_3 to AlN [42]. In order to evaluate the effects of carbon content on the synthesis of spherical AlN particles, the raw powder mixtures with 5 wt.% CaF_2 and various C/Al_2O_3 mole ratios (2.5, 3.0, 4.0, and 5.0) were used, and the CRN process was conducted under the N_2 pressure of 1 MPa and at different temperatures for 2 h.

Figure 8 shows the relationship between the AlN conversion fraction and the C/Al_2O_3 mole ratio at 1500 and 1800°C, respectively. At 1500°C, no samples achieved full nitridation. When the mole ratio of C to Al_2O_3 was 3.0, namely, the theoretical value of the CRN reaction, a highest AlN conversion fraction of ~79% was obtained, while a lower or higher C/Al_2O_3 mole ratio tended to reduce the AlN conversion fraction. As discussed, the formation and nitridation process of liquid Ca-aluminates played a crucial role in the CRN process. When the carbon content was insufficient, the contact interface between carbon and Ca-aluminates decreased. As a consequence, the nitridation rate of Ca-aluminates was reduced, leading to the decrease of the AlN conversion fraction. On the other hand, when the ratio of C to Al_2O_3 exceeded the theoretical value, the excessive carbon tended to hinder the contact between CaF_2 and Al_2O_3. The formation rate of Ca-aluminates was decreased correspondingly, resulting in the low AlN conversion fraction as well.

In addition, it can also be observed from **Figure 8** that the full AlN conversion occurred for the samples with the C/Al_2O_3 mole ratios of 3.0, 4.0, and 5.0 at 1800°C. As for the sample with the C/Al_2O_3 mole ratio of 2.5, a small amount of

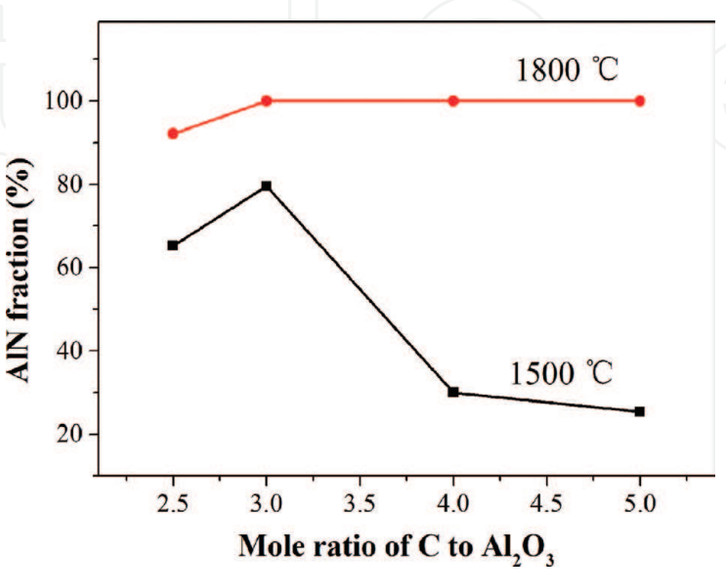

Figure 8.
Relationship between the AlN conversion fraction and the mole ratio of the C/Al_2O_3 mole ratio at 1500 and 1800°C [29].

Al_2O_3 still existed in the system due to the lack of carbon black. The SEM images of all samples synthesized at 1800°C were shown in **Figure 9**.

When the carbon content was less than the theoretical value, many large sintering aggregates could be observed (**Figure 9a**). As increasing the carbon content, the large aggregates gradually disappeared, while the particle size significantly decreased. As known, the growth of particles was not only affected by their growth rate but also restricted by external growth space. When insufficient carbon black was used, the residual carbon black in the late stage was scare. Thus, the AlN particles were likely to contact each other, promoting the formation of large particles and hard aggregates. When the carbon content was excessive, a large amount of unreacted carbon dispersed between AlN particles, which enlarged the migration distance of small particles to AlN nucleus, and limited the growth space of AlN. As a result, AlN powders with smaller particle size were obtained.

2.7 Effects of additive types

In Sections 2.1–2.6, CaF_2 was selected as the typical additive to synthesize spherical AlN fillers by the CRN method. Actually, many single or composite compounds can be used as additives to promote the enhancement of the nitridation rate and the formation of the spherical morphology of AlN particles [37, 43–46]. These compounds have the same characteristic that they can react with Al_2O_3 to produce low-melting liquid aluminates at a relatively low temperature. However, different kinds of additives showed a slight different effect on the nitridation process and the product morphology. **Table 2** shows the powder mixtures with different additive types that the authors previously investigated. The CRN process was carried out at 1400–1800°C and under the N_2 pressure of 1 MPa for 2 h. The influence of additive types on the AlN conversion fraction was summarized in **Table 3**.

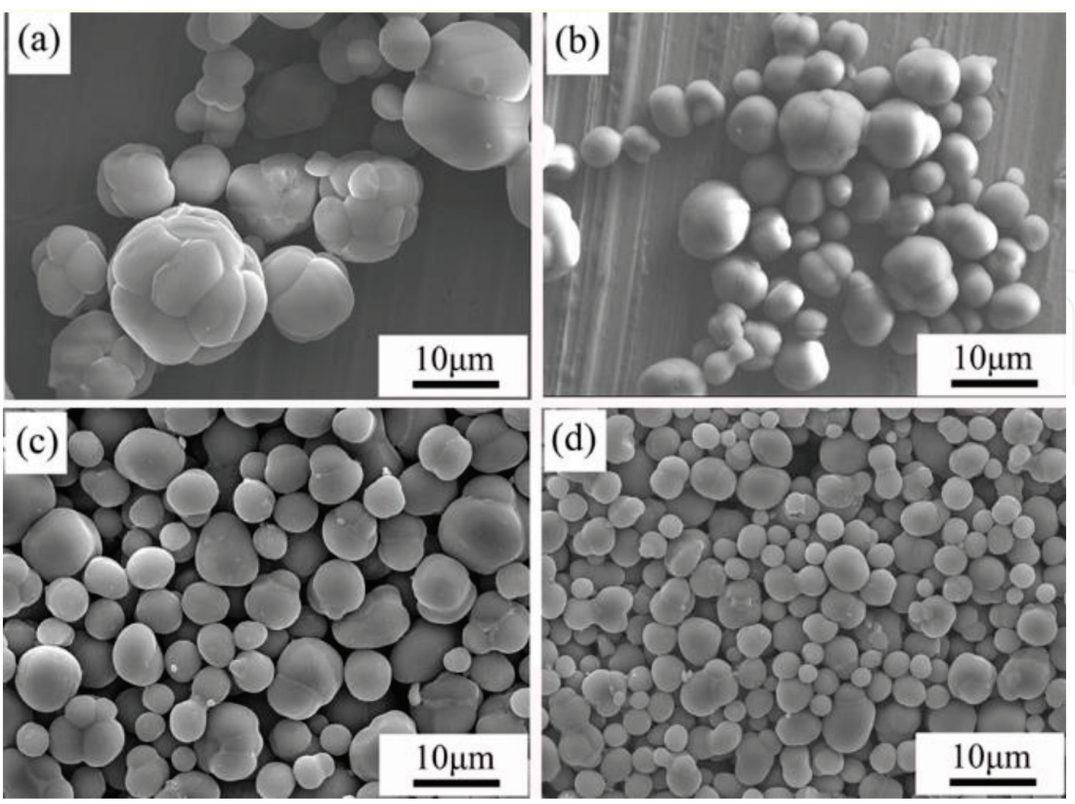

Figure 9.
SEM images of the AlN particles synthesized at 1800°C from samples with various C/Al_2O_3 mole ratios: (a) 2.5, (b) 3.0, (c) 4.0, and (d) 5.0 [29].

Samples	Formulation (in wt.%)				
	Al_2O_3	C	CaF_2	Y_2O_3	YF_3
AP	66.7	33.3	—	—	—
ACF	63.3	31.7	5.0	—	—
AYO	63.3	31.7	—	5.0	—
ACFYO	63.3	31.7	3.0	2.0	—
ACFYF	63.3	31.7	3.0	—	2.0

Table 2.
Compositions of the investigated powder mixtures [32].

Samples	AlN conversion fraction (%)				
	1400°C	1500°C	1600°C	1700°C	1800°C
AP	1.78	42.94	96.02	100.00	100.00
ACF	13.96	32.85	100.00	100.00	100.00
AYO	11.21	67.48	100.00	100.00	100.00
ACFYO	10.70	50.45	100.00	100.00	100.00
ACFYF	35.60	75.62	100.00	100.00	100.00

Table 3.
The AlN conversion fraction at different temperatures for the investigated samples [32].

At 1400°C, all samples with additives showed a higher AlN conversion fraction than that of without additives, further indicating additives favored for the nitridation process. However, it should be noted that the sample ACF showed a lower AlN fraction than AP at 1500°C. This was mainly because most of CaF_2 melts to the liquid phase due to the general melting point of 1418°C. As a result, excessive CaF_2 liquid wrapped on the surface of raw materials, hindering the nitridation process. The rest of samples all present higher AlN conversion fraction than that of AP and ACF, in accordance with the order of ACFYF > AYO > ACFYO. The sample ACFYF presented the highest AlN conversion fraction among all samples. According to the studies of Qiao et al. [38], the formation of $(Ca,Y)F_2$ intermediate and the further appearance of liquid Ca-Y-aluminates at a relatively low temperature of 1350°C were the main reasons for achieving the highest nitridation rate for the Al_2O_3-CaF_2-YF_3 system.

Figure 10 further shows the SEM images of the AlN particles synthesized at 1800°C from various samples. As observed, micro-sized spherical AlN fillers were successfully synthesized from all samples, but their morphology and particle size were slightly different, which might be related to the different formation rate and viscosity of liquid aluminates in the process. From the whole, the sample ACF presented the highest individual sphericity and the best uniformity. Although the near-spherical morphology can also be observed in the remaining samples of AYO, ACFYO, and ACFYF, several hard agglomerates cannot be overlooked. **Figure 11** shows the typical morphology of these hard agglomerates. It can be seen that many compounds precipitated on the particle surface and the neck of sinter particles, which were identified as Y-aluminates by EDS analysis. This indicated that Y-containing compounds could not volatilize as Ca-containing compounds after the CRN reaction, but deposited in the system in the form of precipitates.

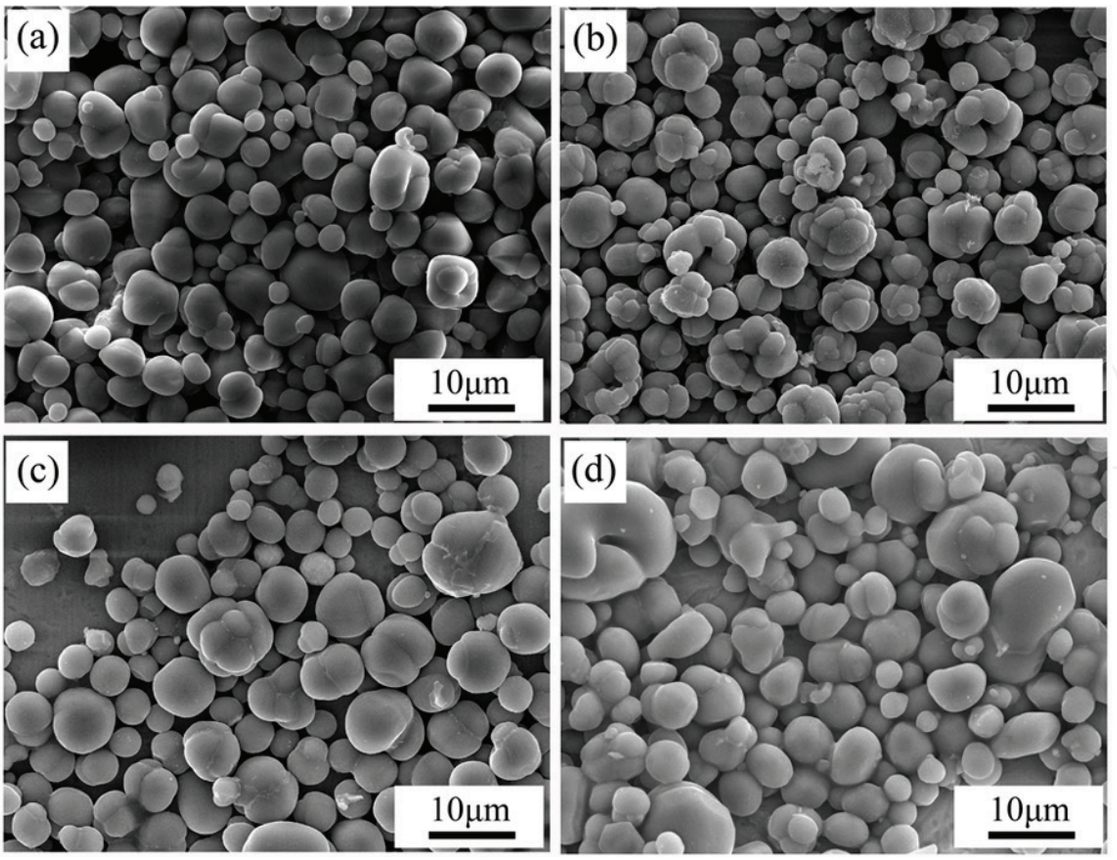

Figure 10.
SEM images of the AlN particles synthesized at 1800°C from samples with various kinds of additives: (a) ACF, (b) AYO, (c) ACFYO, and (d) ACFYF [32].

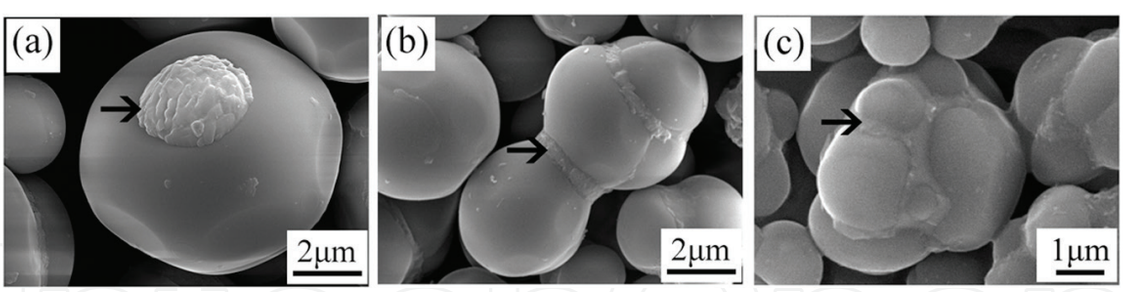

Figure 11.
SEM images of typical microstructures showing Y-aluminate compounds in the sample ACY5 after treatment at 1800°C for 2 h [32].

The appearance of these agglomerates was mainly related to the addition of Y_2O_3. According to other studies [47], in the CRN process, the additive Y_2O_3 firstly reacted with Al_2O_3 to form Y-aluminates, which were further reacted with carbon and N_2 to form AlN based on the following equations:

$$Al_2O_3(s) + Y_2O_3(s) \rightarrow Y\text{-aluminates}(l) \quad (5)$$

$$Y\text{-aluminates}(l) + C(s) + N_2(g) \rightarrow AlN(s) + CO(g) + Y\text{-compounds} \quad (6)$$

When the reaction temperature was high enough or the time was long enough, the Y-aluminates could be reduced completely to Y_2O_3:

$$\text{Y–aluminates (l)} + C(s) + N_2(g) \rightarrow AlN(s) + CO(g) + Y_2O_3(s) \quad (7)$$

According to the studies of sintering AlN ceramics, the existence of these Y-aluminates tended to hinder the connection between AlN grains, leading to the decrease of thermal conductivity of AlN products [48]. However, direct experimental evidence was still necessary for the spherical AlN fillers.

3. Formation mechanism of micro-size spherical AlN fillers

In the above section, we summarized the influence of synthetic parameters on the morphology of final AlN products. It can be concluded that high N_2 pressure, suitable additives, and appropriate reaction temperature were essential to synthesize the micro-sized spherical AlN fillers. Compared with the traditional CRN method, the as-synthesized AlN fillers exhibited two main obvious morphological changes: the growth of the particle size and the sphericity of the particle shape. In this section, we will discuss the formation mechanism of the two morphological changes based on the experimental results.

3.1 Growth mechanism of the AlN particle size

In the process of carbothermal synthesis of spherical AlN fillers, two typical processes occurred: the reaction between Al_2O_3 and additives to form the liquid aluminates and the further reduction and nitridation of aluminates to produce AlN. After formation, the process of AlN particles enlargement could be divided into three stages: nucleation, growth, and coarsening [49]. First, AlN was nucleated in the liquid aluminates, and the number of AlN grains was continuously increased. After that, the newly generated AlN grew on the basis of crystal nucleus, and the AlN particle size was continuously improved. Finally, as the reaction entered the later stage, the small AlN particles were constantly swallowed by the large particles, leading to the rearrangement and coarsening of AlN particles. Therefore, the AlN particle size was determined jointly by the three stages. The low nucleation rate, high growth rate, and high coarsening rate were all advantageous to obtain the AlN fillers with a large particle size.

As demonstrated, the elevated N_2 pressure favored the formation of AlN granules with a large particle size. Under a high N_2 pressure, the release of CO vapor was inhibited, becoming a barrier to limit the contact between Al_2O_3 and N_2. As a result, the AlN nucleation rate was significantly decreased, resulting in a large particle size.

The AlN growth rate was mainly influenced by the formation and nitridation rate of liquid aluminates. In general, when the nucleation rate and holding time were constant, the fast growth rate meant that AlN particles stayed longer in the coarsening stage, which was conducive to the particle size growth. For example, both the small CaF_2 particle size and high reaction temperature could accelerate the formation rate of aluminates, enhancing the AlN growth rate and further promoting the appearance of large AlN particles.

In the later stage of the reaction, the coarsening rate played a decisive role in the final particle size. Since small particles had higher interface energy, they were more easy to be swallowed by the large particles in order to reduce the overall energy of the system, leading to the growth of the AlN particle size. Therefore, the coarsening stage could be considered as the process of interface migration, and the coarsening rate was affected by the reaction time, temperature, and the difficulty of interface migration.

It could be easily understood that longer reaction time meant longer coarsening stage, hence larger particles were more easy to be obtained. However, it should be noticed that too long reaction time could lead to the complete disappearance of small particles, and the interface migration required much more energy than the system could provide. Thus, the growth of the particle size was not that obvious, as demonstrated in Section 2.5.

High reaction time tended to accelerate the rate of interface migration, promoting the growth of the particle size as well. In addition, when more liquid aluminates existed in the system, it got much easier for small particles to migrate to large particles, so the coarsening rate was significantly increased. This can well explain why more CaF_2 content resulted in a larger particle size in Section 2.2.

Moreover, the final particle size was also influenced by the dispersion of second-phase particles. As demonstrated in Section 2.6, excessive carbon black could become the barriers for small particles to large particles. The external growth space of AlN particles were limited, leading to the small AlN particle size.

In summary, the particle size of the as-synthesized AlN fillers was influenced by a variety of synthetic parameters. In the preparation process of the raw materials, decreasing the additive particle size, increasing the additive content, and decreasing the amount of the carbon black all could lead to the increase of the AlN particle size. Additionally, using a high N_2 gas pressure, increasing the reaction temperature and prolonging the holding time in the CRN reaction process could result in larger AlN particles as well.

3.2 Sphericity mechanism of the AlN particle shape

According to the comprehensive investigations in Section 2, it can be concluded that the amount and distribution of liquid aluminates were important for the formation of the spherical AlN morphology. Based on the crystal growth theory [41], crystals preferred to grow into the lowest energy state. When there were no liquids in the system, the AlN morphology was mainly determined by the internal intrinsic structure. Thus, AlN particles tended to grow in the angular morphology to achieve the most stable state of energy. However, when additives were used in the CRN process, AlN was nucleated in the liquid aluminates, and thus its morphology was consequentially influenced by the external liquid phase environment. The solid AlN and liquid phase constituted a common system, and hence the lowest solid-liquid interface energy became the main driving force for the growth of AlN. Compared with the angular morphology, spherical particles showed the least specific surface area and the corresponding lowest solid-liquid interface energy. Therefore, AlN tended to grow into the spherical morphology with the aid of liquid Ca-aluminates.

Based on the above inference, only when the AlN particles were completely wrapped in the liquids during the growth stage, the spherical morphology could be obtained. Thus, both the low liquid content and the fast AlN growth rate could lead to the disappearance of the solid-liquid interface and the difficulty to form the spherical shape. For example, when a low N_2 pressure was used, the AlN growth rate was significantly increased so that the AlN particles could not be completely wrapped by the liquids, resulting in the poor sphericity. In addition, the low reaction temperature and the little additive content both led to the small liquid content, thus the spherical AlN particles could not be obtained as well. It can be concluded that the elevated N_2 pressure, suitable additives, and relatively high reaction temperature greatly favored for carbothermally synthesizing AlN particles with a smooth spherical morphology.

4. Conclusion and perspective

In conclusion, this chapter presents the recent advances on the carbothermal synthesis of spherical AlN fillers. The influence of various synthetic parameters on the morphology and particle size of final products is summarized. During the CRN process, the elevated N_2 gas pressure favored the growth of the particle size and the formation of the uniform spherical morphology, but hampered the nitridation rate. The relatively high reaction temperature could result in the increasing nitridation rate, the growth of the particle size, and the sphericity of AlN particles, but a too high temperature above 1900°C was not beneficial for the spherical morphology due to the decreasing liquid content. Prolonging the reaction time properly was also conducive to the formation of large spherical AlN particles. As for the raw materials, increasing the additive content tended to enhance the sphericity and particle size of AlN particles; excessive carbon black reduced the nitridation rate and particle size, but increased the sphericity of AlN particles; the use of the additive with a large particle size could slow down the nitridation rate and reduce the AlN particle size.

In summary, the liquid aluminates forming from the reaction between Al_2O_3 and additives played an important role in the carbothermal synthesis of spherical AlN fillers by improving the nitridation rate, increasing the particle size, and promoting the formation of smooth spherical appearance. The condition that AlN particles were completely wrapped with liquid aluminates during the growth stage was necessary for the spherical morphology.

Although the micron-sized spherical AlN particles, which showed great potentiality to be used as fillers, were successfully synthesized by the CRN method, further research is still necessary aiming at evaluating the actual thermal conductivity of the AlN fillers and the performance of the as-prepared thermal interface materials.

Acknowledgements

The authors gratefully acknowledge the financial support from the National Key R&D Program of China (No. 2017YFB0310301) and National Natural Science Foundation of China (No. 51602017).

Conflict of interest

The authors declare no conflict of interest.

Author details

Qi Wang[1*], Kexin Chen[2] and Wenbin Cao[1]

1 Department of Inorganic Nonmetallic Materials, School of Materials Science and Engineering, University of Science and Technology Beijing, Beijing, China

2 State Key Laboratory of New Ceramics and Fine Processing, School of Materials Science and Engineering, Tsinghua University, Beijing, China

*Address all correspondence to: wangqi15@ustb.edu.cn

References

[1] Chung DDL. Thermal interface materials. Journal of Materials Engineering and Performance. 2001;**10**:56-59. DOI: 10.1361/105994901770345358

[2] Chen H, Ginzburg VV, Yang J, Yang Y, Liu W, Huang Y, et al. Thermal conductivity of polymer-based composites: Fundamentals and applications. Progress in Polymer Science. 2016;**59**:41-85. DOI: 10.1016/j.progpolymsci. 2016.03.001

[3] Afzal A, Siddiqi HM, Iqbal N, Ahmad Z. The effect of SiO_2 filler content and its organic compatibility on thermal stability of epoxy resin. Journal of Thermal Analysis and Calorimetry. 2013;**111**:247-252. DOI: 10.1007/s10973-012-2267-9

[4] Procter P, Solc J. Improved thermal conductivity in microelectronic encapsulants. In: Proceedings of the 41st Electronic Components & Technology Conference; 11-16 May 1991; Atlanta. New York: IEEE; 1991. pp. 835-842

[5] Huang X, Jiang P, Tanaka T. A review of dielectric polymer composites with high thermal conductivity. IEEE Electrical Insulation Magazine. 2011;**27**:8-16. DOI: 10.1109/MEI.2011.5954064

[6] Varlow BR, Robertson J, Donnelly KP. Nonlinear fillers in electrical insulating materials. IET Science, Measurement and Technology. 2007;**1**:96-102. DOI: 10.1049/iet-smt:20060007

[7] Kozako M, Okazaki Y, Hikita M, Tanaka T. Preparation and evaluation of epoxy composite insulating materials toward high thermal conductivity. In: Proceedings of the 10th IEEE International Conference on Solid Dielectrics; 4-9 July 2010; Potsdam. New York: IEEE; 2010. pp. 1-4

[8] Sim LC, Ramanan SR, Ismail H, Seetharamu KN, Goh TJ. Thermal characterization of Al_2O_3 and ZnO reinforced silicone rubber as thermal pads for heat dissipation purposes. Thermochimica Acta. 2005;**430**:155-165. DOI: 10.1016/j.tca.2004.12.024

[9] Zhou W, Qi S, Tu C, Zhao H, Wang C, Kou J. Effect of the particle size of Al_2O_3 on the properties of filled heat-conductive silicone rubber. Journal of Applied Polymer Science. 2007;**104**:1312-1318. DOI: 10.1002/app.25789

[10] Donnay M, Tzavalas S, Logakis E. Boron nitride filled epoxy with improved thermal conductivity and dielectric breakdown strength. Composites Science and Technology. 2015;**110**:152-158. DOI: 10.1016/j.compscitech.2015.02.006

[11] Xu Y, Chung DDL. Increasing the thermal conductivity of boron nitride and aluminum nitride particle epoxy-matrix composites by particle surface treatments. Composite Interfaces. 2000;**7**:243-256. DOI: 10.1163/156855400750244969

[12] Furuya K, Munakata F, Matsuo K, Akimune Y, Ye J, Okada A. Microstructural control of b-silicon nitride ceramics to improve thermal conductivity. Journal of Thermal Analysis and Calorimetry. 2002;**69**:873-879. DOI: 10.1023/A:1020660006988

[13] Slack GA. Nonmetallic crystals with high thermal conductivity. Journal of Physics and Chemistry of Solids. 1973;**34**:321-335. DOI: 10.1016/0022-3697(73)90092-9

[14] Slack GA, Tanzilli RA, Pohl RO, Vandersande JW. The intrinsic thermal conductivity of AIN. Journal of Physics and Chemistry of

Solids. 1987;**48**:641-647. DOI: 10.1016/0022-3697(87)90153-3

[15] Ohashi M, Kawakami S, Yokogawa Y, Lai G-C. Spherical aluminum nitride fillers for heat-conducting plastic packages. Journal of the American Ceramic Society. 2005;**88**:2615-2618. DOI: 10.1111/j.1551-2916.2005.00456.x

[16] Zhou Y, Wang H, Wang L, Yu K, Lin Z, He L. Fabrication and characterization of aluminum nitride polymer matrix composites with high thermal conductivity and low dielectric constant for electronic packaging. Materials Science and Engineering B. 2012;**177**:892-896. DOI: 10.1016/j.mseb.2012.03.056

[17] Burger N, Laachachi A, Ferriol M, Lutz M, Toniazzo V, Ruch D. Review of thermal conductivity in composites: Mechanisms, parameters and theory. Progress in Polymer Science. 2016;**61**:1-28. DOI: 10.1016/j.progpolymsci.2016.05.001

[18] Chon CH, Kihm KD, Lee SP, Choi SUS. Empirical correlation finding the role of temperature and particle size for nanofluid (Al_2O_3) thermal conductivity enhancement. Applied Physics Letters. 2005;**87**:153107. DOI: 10.1063/1.2093936

[19] Fan ZY, Newman N. Experimental determination of the rates of decomposition and cation desorption from AlN surfaces. Materials Science and Engineering B. 2001;**87**:244-248. DOI: 10.1016/S0921-5107(01)00720-6

[20] Chowdhury SA, Maiti HS, Biswas S. Synthesis of spherical Al_2O_3 and AlN powder from C@Al_2O_3 composite powder. Journal of Materials Science. 2006;**41**:4699-4705. DOI: 10.1007/s10853-006-0039-2

[21] Suehiro T, Tatami J, Meguro T, Matsuo S, Komeya K. Morphology-retaining synthesis of AlN particles by gas reduction–nitridation. Materials Letters. 2002;**57**:910-913. DOI: 10.1016/S0167-577X(02)00894-7

[22] Wang Q, Ge Y, Sun S, Kuang J, Ferreira JMF, Cao W. Preparation of dense spherical AlN fillers by aqueous granulation and post-sintering process. Ceramics International. 2017;**43**:2027-2032. DOI: 10.1016/j.ceramint.2016.10.171

[23] Wang Q, Olhero SM, Ferreira JMF, Cui W, Chen K, Xie Z. Hydrolysis control of AlN powders for the aqueous processing of spherical AlN granules. Journal of the American Ceramic Society. 2013;**96**:1383-1389. DOI: 10.1111/jace.12288

[24] Selvaduray G, Sheet L. Aluminium nitride: Review of synthesis methods. Materials Science and Technology. 1993;**9**:463-473. DOI: 10.1179/mst.1993.9.6.463

[25] Wu H, Qin M, Chu A, Wan Q, Cao Z, Liu Y, et al. AlN powder synthesis by sodium fluoride-assisted carbothermal combustion. Ceramics International. 2014;**40**:14447-14452. DOI: 10.1016/j.ceramint.2014.07.014

[26] Qin M, Du X, Wang J, Humail IS, Qu X. Influence of carbon on the synthesis of AlN powder from combustion synthesis precursors. Journal of the European Ceramic Society. 2009;**29**:795-799. DOI: 10.1016/j.jeurceramsoc.2008.07.019

[27] Wang H, Yang Q, Jia G, Lei R, Wang S, Xu S. Influence of yttrium dopant on the synthesis of ultrafine AlN powders by CRN route from a sol–gel low temperature combustion precursor. Advanced Powder Technology. 2014;**25**:450-456. DOI: 10.1016/j.apt.2013.07.008

[28] Yamakawa T, Tatami J, Wakihara T, Komeya K, Meguro T, MacKenzie KJD, et al. Synthesis of AlN nanopowder from γ-Al_2O_3 by

reduction–nitridation in a mixture of NH_3–C_3H_8. Journal of the American Ceramic Society. 2006;**89**:171-175. DOI: 10.1111/j.1551-2916.2005.00693.x

[29] Wang Q, Cao W, Kuang J, Jiang P. Spherical AlN particles synthesized by the carbothermal method: Effects of reaction parameters and growth mechanism. Ceramics International. 2018;**44**:4829-4834. DOI: 10.1016/j.ceramint.2017.12.071

[30] Wang Q, Cui W, Ge Y, Chen K, Xie Z. Preparation of spherical AlN granules directly by carbothermal reduction-nitridation method. Journal of the American Ceramic Society. 2015;**98**:392-397. DOI: 10.1111/jace.13324

[31] Wang Q, Ge Y, Cui W, Chen K, Ferreira JMF, Xie Z. Carbothermal synthesis of micro-scale spherical AlN granules with CaF2 additive. Journal of Alloys and Compounds. 2016;**663**:823-828. DOI: 10.1016/j.jallcom.2015.12.178

[32] Wang Q, Ge Y, Kuang J, Jiang P, Liu W, Cao W. Effects of additives on the synthesis of spherical aluminum nitride granules by carbothermal reduction-nitridation process. Journal of Alloys and Compounds. 2017;**696**:220-225. DOI: 10.1016/j.jallcom.2016.11.252

[33] Wang Q, Kuang J, Jiang P, Cao W. Carbothermal synthesis of spherical AIN particles using sucrose as carbon source. Ceramics International. 2018;**44**:3480-3483. DOI: 10.1016/j.ceramint.2017.11.056

[34] Forslund B, Zheng J. Carbothermal synthesis of aluminium nitride at elevated nitrogen pressures, part I: Effect of process parameters on conversion rate. Journal of Materials Science. 1993;**28**:3125-3131. DOI: 10.1007/BF00354225

[35] Forslund B, Zheng J. Carbothermal synthesis of aluminium nitride at elevated nitrogen pressures, part II: Effect of process parameters on particle size and porphology. Journal of Materials Science. 1993;**28**:3132-3136. DOI: 10.1007/BF00354226

[36] Ide T, Komeya K, Meguro T, Tatami J. Synthesis of AlN powder by Carbothermal reduction-Nitridation of various Al_2O_3 powders with CaF_2. Journal of the American Ceramic Society. 1999;**82**:2993-2998. DOI: 10.1111/j.1151-2916.1999.tb02193.x

[37] Molisani AL, Yoshimura HN. Low-temperature synthesis of AlN powder with multicomponent additive systems by carbothermal reduction–nitridation method. Materials Research Bulletin. 2010;**45**:733-738. DOI: 10.1016/j.materresbull.2010.02.012

[38] Qiao L, Zhou H, Fu R. Thermal conductivity of AlN ceramics sintered with CaF_2 and YF_3. Ceramics International. 2003;**29**:893-896. DOI: 10.1016/S0272-8842(03)00033-6

[39] Komeya K, Kitagawa I, Meguro T. Effect of Ca-compound addition on synthesis of AlN powder by carbothermal reduction-nitridation method. Journal of the Ceramic Society of Japan. 1994;**102**:670-674. DOI: 10.2109/jcersj.102.670

[40] Xiong Y, Wang H, Fu Z. Transient liquid-phase sintering of AlN ceramics with CaF_2 additive. Journal of the European Ceramic Society. 2013;**33**:2199-2205. DOI: 10.1016/j.jeurceramsoc.2013.03.024

[41] Cahn JW. Theory of crystal growth and interface motion in crystalline materials. Acta Metallurgica. 1960;**8**:554-562. DOI: 10.1016/0001-6160(60)90110-3

[42] Cho YW, Charles JA. Synthesis of nitrogen ceramic povvders by carbothermal reduction and nitridation, part 3 aluminium nitride. Materials

Science and Technology. 1991;**7**:495-504. DOI: 10.1179/mst.1991.7.6.495

[43] Kume S, Yasuoka M, Lee S-K, Kan A, Ogawa H, Watari K. Dielectric and thermal properties of AlN ceramics. Journal of the European Ceramic Society. 2007;**27**:2967-2971. DOI: 10.1016/j.jeurceramsoc.2006.11.023

[44] Nakano H, Watari K, Hayashi H, Urabe K. Microstructural characterization of high-thermal-conductivity aluminum nitride ceramic. Journal of the American Ceramic Society. 2002;**85**:3093-3095. DOI: 10.1111/j.1151-2916.2002.tb00587.x

[45] Hundere AM, Einarsrud M-A. Microstructural development in AlN (YF_3) ceramics. Journal of the European Ceramic Society. 1997;**17**:873-878. DOI: 10.1016/S0955-2219(96)00199-9

[46] Liu Y, Zhou H, Qiao L, Wu Y. Low-temperature sintering of aluminum nitride with YF_3–CaF_2 binary additive. Journal of Materials Science Letters. 1999;**18**:703-704. DOI: 10.1023/A:1006692111736

[47] Ide T, Komeya K, Tatami J, Meguro T, Naito M, Hotta T. Effect of Y_2O_3 addition on synthesis of AlN powder by carbothermal reduction-nitridation of Al_2O_3. Journal of the Ceramic Society of Japan. 2001;**109**:372-375. DOI: 10.2109/jcersj.109.1268_372

[48] Virkar AV, Jackson TB, Cutler RA. Thermodynamic and kinetic effects of oxygen removal on the thermal conductivity of aluminum nitride. Journal of the American Ceramic Society. 1989;**72**:2031-2042. DOI: 10.1111/j.1151-2916.1989.tb06027.x

[49] Chen IW, Davenport A, Wang L. Accelerated precipitate coarsening due to a concomitant secondary phase transformation. Acta Materialia. 2003;**51**:1691-1703. DOI: 10.1016/S1359-6454(02)00570-0